

A decagallane(6) cluster $\text{Ga}_{10}[\text{Si}(\text{CMe}_3)_3]_6$ with an unprecedented structure†

Gerald Linti^{*a} and Annekathrin Seifert^b

Received 20th February 2008, Accepted 18th April 2008

First published as an Advance Article on the web 2nd June 2008

DOI: 10.1039/b802959h

The decagallane(6) $\text{Ga}_{10}\text{R}'_6$ [$\text{R}' = \text{Si}(\text{CMe}_3)_3$] adopts a quite unusual structure, which might be described as being derived from a pentagonal bipyramidal core, which is threefold capped. An alternative description is that of a *conjuncto*-cluster. The structure of the anionic cluster $[\text{Ga}_{10}\text{R}'_6]^-$ as well as that of $\text{Ga}_{10}\text{R}''_6$ [$\text{R}'' = \text{Si}(\text{SiMe}_3)_3$] are described as being built of fused octahedra. Thus, this family of decagallanes is unique in showing structural isomers in the cluster core, giving hints to the pathways of formation of these clusters, too. The novel cluster compound is characterized by X-ray crystallography. Isomeric decagallanes(6) and structural changes on reduction are studied by DFT methods.

Introduction

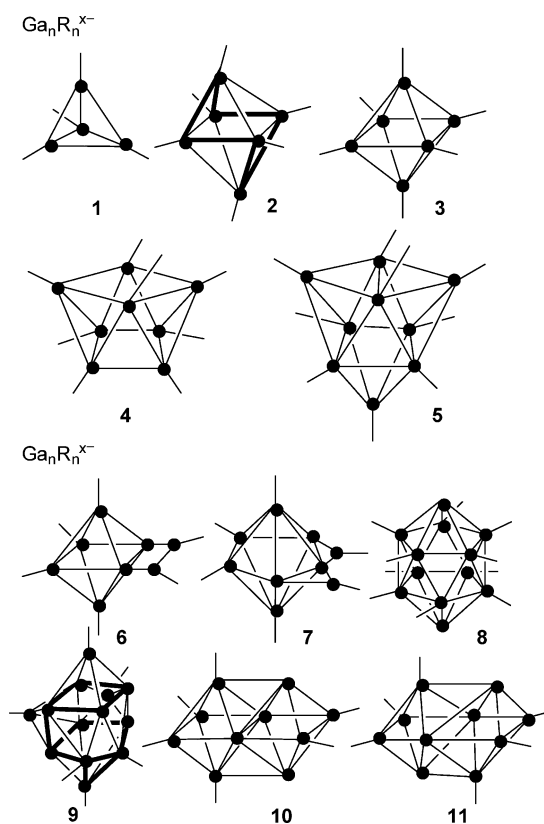
The clusters of gallium, characterized until now, can be divided into two series¹ (Scheme 1). The first, comprising compounds of the type $[\text{Ga}_n\text{R}_m]^{x-}$ ($x = 0, 1, 2; n = 4, 6, 8, 9$), might be looked upon as classical polyhedral clusters. Examples are Ga_4R_4 **1** [$\text{R} = \text{C}(\text{SiMe}_3)_3$],² Ga_6R_6 **2** [$\text{R} = \text{Si}(\text{SiMe}_3)_3$],³ Ga_6R_6 **3** [$\text{R} = \text{Si}(\text{CMe}_3)_3$],⁴ *precloso*- $\text{Ga}_6[\text{SiMe}(\text{SiMe}_3)_2]_6$ **2**,⁵ *closo*- $[\text{Ga}_6\{\text{Si}(\text{CMe}_3)_3\}_4(\text{CH}_2\text{Ph})_2]^{2-}$ **3**,⁵ the formally *closo* cluster $[\text{Ga}_8(\text{fluorenyl})_8]^{2-}$ **4**,⁶ and *precloso*- $[\text{Ga}_9(\text{CMe}_3)_9]^{5.7.8}$ **5**.^{7,8} The dianionic compounds fit the Wade–Williams rules.^{9–14}

Tetragallanes(4) **1** with a tetrahedral structure and four skeleton electron pairs are cluster compounds, where the cluster bonding is described as four three-centre two-electron (3c2e)-bonds. **3** is an octahedral *closo*-cluster with seven skeleton electron pairs, while **2** has only six cluster electron pairs. Here a Jahn–Teller distortion of a regular polyhedron is observed.

The second series are gallium-rich cluster compounds $[\text{Ga}_n\text{R}_m]^{x-}$ ($m < n$). Some prominent examples are $[\text{Ga}_8\{\text{Si}(\text{CMe}_3)_3\}_6]^{x-}$ ($x = 0, 2$) **6**,¹⁵ $[\text{Ga}_9\{\text{Si}(\text{SiMe}_3)_3\}_6]^{x-}$ ($x = 0, 2$) **7**,¹⁶ $[\text{Ga}_{12}\text{fluorenyl}_{10}]^{2-}$ **8**,¹⁷ and $[\text{Ga}_{13}\{\text{Si}(\text{CMe}_3)_3\}_6]^{x-}$ **9**.¹⁸ Even higher clusters with up to 84 gallium atoms are known, for a recent review see ref. 19.

Whilst **6** and **7** might be understood as *closo*-clusters with a six or seven vertex core, respectively, which are substituted by four R groups and two GaR units, the higher clusters show structures which resemble sectors of structures observed in modifications of gallium.¹

Of special interest are Ga_{22} clusters. In addition to the $[\text{Ga}_{22}\text{R}_8]$ clusters [$\text{R} = \text{Si}(\text{SiMe}_3)_3$,²⁰ $\text{Ge}(\text{SiMe}_3)_3$,²¹ $\text{Si}(\text{CMe}_3)_3$,²²], Ga_{22} clusters with different numbers of substituents and consequently different core structures are known. These are $[\text{Ga}_{22}\{\text{N}(\text{SiMe}_3)_2\}_{10}]^{2-}$,²³ $[\text{Ga}_{22}\{\text{N}(\text{SiMe}_3)_2\}_{10}\text{Br}_{10}]^{2-}$ ²⁴ and $\text{Ga}_{22}(\text{PtBu}_2)_{12}$.²⁵ The first with eight and ten substituents have core



Scheme 1 Survey of gallium cluster compounds of types $[\text{Ga}_n\text{R}_m]^{x-}$ and $[\text{Ga}_n\text{R}_m]^{x-}$.

structures of 14 and 12 gallium atoms, respectively, which are surrounded by eight or ten GaR units. The Ga_{14} core is a centered Ga_{13} polyhedron, the Ga_{12} core a centered Ga_{11} polyhedron. In contrast, those clusters which have more substituents possess icosahedral Ga_{12} cores without a central atom. This structural diversity seemed to be unique in cluster chemistry.

We want to focus now on Ga_{10} cluster compounds. Two clusters $[\text{Ga}_{10}\text{R}_6]^{n-}$ have been prepared.¹⁸ A neutral $\text{Ga}_{10}[\text{Si}(\text{SiMe}_3)_3]_6$ cluster **10** and an anionic $[\text{Ga}_{10}\{\text{Si}(\text{CMe}_3)_3\}_6]^-$ **11** have cluster cores of fused octahedra. They differ in the distribution of the six substituents on the cluster atoms. That means in **10** a 4/2, in **11**

^aUniversity of Heidelberg, Institute of Inorganic Chemistry, Im Neuenheimer Feld 270, D-69120, Heidelberg, Germany. E-mail: Gerald.linti@aci.uni-heidelberg.de; Fax: +49-6221-546617; Tel: +49-6221-548468

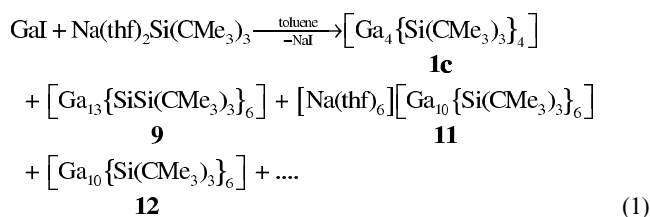
^bAnorganisch-Chemisches Institut, Universität Heidelberg, Im Neuenheimer Feld 270, D-69120, Heidelberg, Germany

† Electronic supplementary information (ESI) available: Table with SEN and plots of MOs for **12a**. CCDC reference number 602531. For ESI or crystallographic data in CIF or other electronic format see DOI: 10.1039/b802959h

a 3/3 distribution of substituents is observed. In **11** the octahedra are severely distorted. Thus, a description of a trigonal antiprism of GaR units with an intercalated Ga₄ ring was used. Here we describe a novel Ga₁₀R₆ cluster with a different cluster structure.

Results and discussion

In the reaction of “GaI”,²⁶ prepared from the elements in an ultrasonic bath, with Na(thf)₂Si(CMe₃)₃,²⁷ several cluster compounds are formed. Recently, we reported on one of the products, namely **11**.¹⁸ In addition, the tetragallane [Ga₄{Si(CMe₃)₃}₄] **1c** is formed. From a toluene solution of the crude products of this reaction black crystals could be isolated, which were analyzed to be co-crystals of clusters **1c** and [Ga₁₀{Si(CMe₃)₃}₆] **12** (eqn (1)).



This reaction involves a lot of redox reactions, leading to the formation of elemental gallium and other cluster compounds like [Ga₁₃{Si(CMe₃)₃}₆] **9** in low yields. In addition various silanes like (Me₃C)₃SiH and [(Me₃C)₃Si]₂ are observed.

1c and **12** crystallize together in prisms of the monoclinic system, space group *Cc* (see Table 1). Here clusters **12** form approximately close packed hexagonal layers with a layer of the tetrahedral cluster **1c** and thf in between. **1c** shows Ga–Ga distances averaging to 253.6 pm [*d*_{GaGa} = 252.2(1)–254.4(1) pm]. This is shorter than reported for **1c** (*d*_{GaGa} = 257.2 pm), crystallized separately.⁴ Thus the tetrahedron is slightly compressed, which might be due to incorporation in the crystal structure of **12**.

Table 1 Crystallographic data for **12·1c**

Empirical formula	Ga ₁₀ Si ₆ C ₇₂ H ₁₆₂ ·Ga ₄ Si ₄ C ₄₈ H ₁₀₈ ·OC ₄ H ₈
<i>M_r</i> /g mol ⁻¹	3042.4
<i>T</i> /K	150
<i>λ</i> /Å	0.71073
Crystal system	Monoclinic
Space group	<i>Cc</i>
<i>a</i> /pm	4727(1)
<i>b</i> /pm	2117.4(4)
<i>c</i> /pm	1666.3(3)
<i>β</i> /°	107.54(3)
<i>V</i> /Å ³	15903(5)
<i>Z</i>	4
<i>ρ</i> _{calc} /g cm ⁻³	1.27
<i>μ</i> /mm ⁻¹	2.44
<i>F</i> (000)	6416
<i>2θ</i> range/°	3–45
Index range	±
	50, ±22, ±17
Parameters	1427
Reflections, collected	44359
Reflections, unique	20193 (<i>R</i> _{int} = 0.0524)
GOOF on <i>F</i> ²	0.883
Final <i>R</i> indices [<i>I</i> > 2σ(<i>I</i>)] ^a	<i>R</i> ₁ = 0.046, <i>wR</i> ₂ = 0.095
<i>R</i> indices (all data)	<i>R</i> ₁ = 0.069, <i>wR</i> ₂ = 0.10

^a Weighting scheme: *w* = 1/[σ²(*F*_o²) + (0.0504*P*)² + 0.0000*P*] where *P* = (*F*_o² + 2*F*_c²)/3.

The cluster **12** is composed of ten gallium atoms, six of them bearing silyl groups (Fig. 1). The cluster core is difficult to describe, because no regular polyhedron is present. **12** might be viewed as having a flat, distorted pentagonal bipyramidal core of gallium atoms. The equatorial plane exhibits three rather short and two long Ga–Ga distances which are bridged by gallium atoms. That means Ga(8) bridges the Ga(1)–Ga(5) edge, with Ga(8)–Ga distances of 243 pm (averaged). The bridged edge [*d*_{Ga(1)–(5)Ga} = 306 pm] is the longest in this cluster. Alternatively, **12** might be described as made up of fused Ga₈ and Ga₄ polyhedra, sharing the Ga(1)–Ga(2) edge. DFT calculations (see Table 5) indicate a large three-center bonding contribution to the Ga(1)–Ga(8)–Ga(5) triangle. This is in support of a description of the cluster as a bridged pentagonal bipyramid.

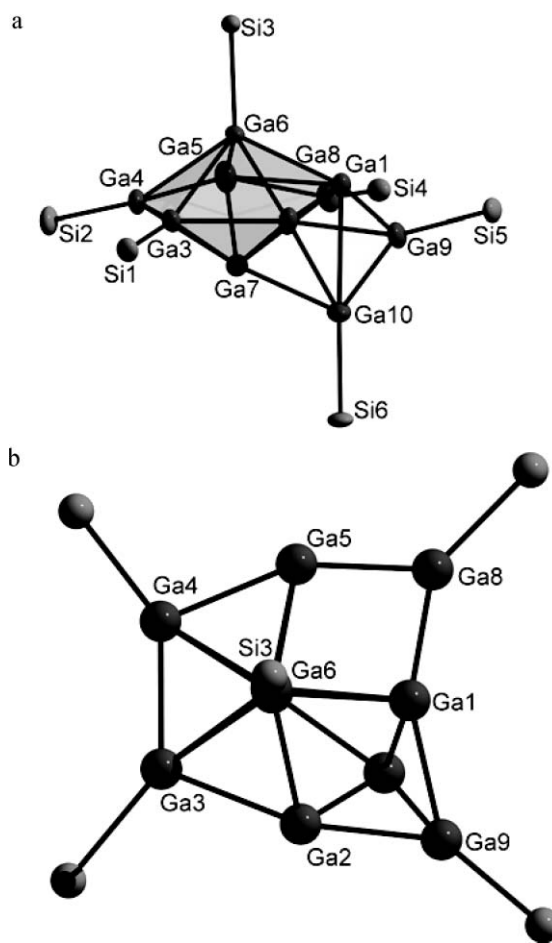


Fig. 1 View of cluster molecule **12**. *tert*-Butyl groups have been omitted for clarity. (a) polyhedral view, (b) view down the Si₃–Ga₆–Ga₇ axis. Selected distances [pm]: Ga(1)–Ga(2) 284.0(1), Ga(1)–Ga(6) 270.1(1), Ga(1)–Ga(7) 289.1(1), Ga(1)–Ga(8) 244.1(1), Ga(1)–Ga(9) 253.3(1), Ga(1)–Ga(10) 287.8(1), Ga(2)–Ga(3) 256.9(1), Ga(2)–Ga(6) 280.1(1), Ga(2)–Ga(7) 275.6(1), Ga(2)–Ga(9) 246.5(1), Ga(2)–Ga(10) 291.4(1), Ga(3)–Ga(4) 255.1(1), Ga(3)–Ga(6) 277.8(1), Ga(3)–Ga(7) 273.1(1), Ga(4)–Ga(5) 253.4(1), Ga(4)–Ga(6) 278.0(1), Ga(4)–Ga(7) 261.0(1), Ga(5)–Ga(6) 265.2(1), Ga(5)–Ga(7) 267.6(1), Ga(5)–Ga(8) 241.5(1), Ga(6)–Ga(7) 295.3(1), Ga(7)–Ga(10) 252.4(1), Ga(9)–Ga(10) 246.6(1), Ga(3)–Si(1) 249.7(2), Ga(4)–Si(2) 250.2(2), Ga(6)–Si(3) 246.9(2), Ga(8)–Si(4) 242.1(2), Ga(9)–Si(5) 241.0(2), Ga(10)–Si(6) 245.5(2).

The remaining edges in the pentagonal bipyramidal core range between 253.3(1) and 289.1(1) pm. Ga(9) is bridging the long Ga(1)–Ga(2) edge with Ga(9)–Ga distances of 246.5(1) and 253.3(1) pm, respectively. Ga(9) is additionally bonded to Ga(10) [$d_{\text{GaGa}} = 246.6(1)$ pm]. Ga(10) itself is bridging the face Ga(1), Ga(2), Ga(7) unsymmetrically [$d_{\text{GaGa}} = 252.4(1)$ – $291.4(1)$ pm]. The bipyramid is quite flat with a Ga–Ga distance of 295.3(1) pm between the apical atoms. This is similar to the lengths of edges in this cluster and hints to an additional interaction and is consistent with the results of the DFT calculations.

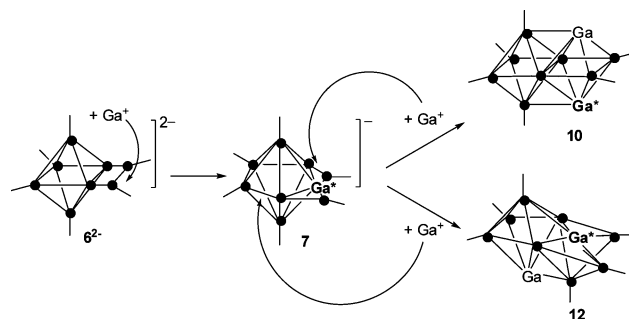
Three gallium atoms, making up one triangular face of this polyhedron, are connected to silicon atoms of Si(CMe₃)₃ groups. The remaining three gallium atoms, which are bonded to silyl groups, are in bridging positions, either bridging an edge or a face. This broad distribution of Ga–Ga distances is typical for gallium rich cluster compounds.¹ The Ga–Si distances show a broad variability, too. The Ga–Si bonds [$d_{\text{GaSi}} = 240.9(2)$ – $245.5(2)$ pm] to the bridging gallium atoms are shorter than the gallium–silicon bonds of the bipyramidal core atoms [$d_{\text{GaSi}} = 246.9(2)$ – $250.2(2)$ pm].

The structure of **12** resembles somewhat that of the nonagallane **7**, in which two R₂Ga units bridge two neighbouring edges of a pentagonal bipyramid with Ga–Ga distances of 234.4(1) and 237.7(1) pm. The edges in the bipyramidal core range between 242.5(1) and 289.8(1) pm. The pentagonal bipyramid is less flat ($d_{\text{GaGa}} = 344$ pm) than that in **12**. **7**¹⁵ can be explained as a *closo*-Ga₇ cluster with four silyl and two bridging R₂Ga substituents.

An electron count for **12**, built formally by 6 R₂Ga units and 4 Ga atoms, is not unambiguous, since it is not obvious which of the bare gallium atoms contribute the usual three orbitals to the cluster skeleton and which provide four orbitals. The usual count would result in eight skeleton electron pairs, which, according to the Wade–Mingos rules,^{9–14} is in line with a three-capped seven vertex polyhedron. Obviously, **12** seems to have far too few skeletal electrons for a polyhedral cluster. Therefore, **12** is not a polyhedral cluster of this type. We find a flattened, irregular polyhedral core with several cappings. The short Ga(6)–Ga(7) distance suggests that the bare vertex atom Ga(7) contributes not only one, but three electrons and four orbitals to the cluster bonding. This should be the case for Ga(1) and Ga(2), too, which would give 11 skeletal pairs for **12**. The structures and electron count in bare indium clusters have been discussed similarly, on the basis of flattening vertices as a result of the contribution of four orbitals to cluster bonding by some of the vertex atoms.^{28,29} Thus, In₁₁^{7–} has three flattened vertices, which allows for 12 skeletal electron pairs, required for a *closo*-cluster.³⁰

A comparison of **12** with the structural isomeric cluster **10** seems appropriate.¹⁸ Here, a description as a three capped cluster is not obvious. Cluster **10** was rationalized as being a *conjuncto*-cluster³¹ according to the Jemmis counting rules.^{32,33} But this implies a different counting of electrons for some of the naked Ga atoms (3 cluster electrons instead of 1), too. According to this, 24 skeleton electrons in **10** allow a *conjuncto* cluster made up of two subpolyhedra; *i.e.* two octahedra in **10**. Therefore, 22 skeleton electrons in **12** are consistent with a tetrahedron and a hexagonal bipyramid (or bridged pentagonal bipyramid). The latter is severely distorted (see above). Obviously, both counting rules roughly give explanations for the structure of this hypoelectronic cluster but are near their limits. Therefore, a forecast of structures on this basis is not possible at all.

Looking for structural analogies (disregarding different R substituents), **10** can be viewed upon as derived from an anionic cluster with a core like **7** by addition of Ga⁺, shown to attack at Ga(*) (Scheme 2). Similarly, **7** might be derived from addition of a Ga⁺ ion to [Ga₈R₆]^{2–}. If Ga⁺ is added to **7** not at the Ga₃(GaR)₂ site but *via* an opposite triangular face, **12** is formed instead of **10**.



Scheme 2 Possible formation pathways for clusters with cores of types **7**, **10** and **12**.

The isomeric, neutral clusters Ga₁₀(SiMe₃)₆ **10a** and **12a** have been studied by DFT-methods (RI-DFT, BP86 functional, def SV(P)-base)³⁴ (Fig. 2 and 3, Tables 2 and 3). **10a**, with a core structure similar to **10**, is the most stable isomer. **12a** is less stable by 56.6 kJ mol^{–1}, based on total electronic energies.

Starting from the calculated structure **12a** the apical Ga atom (Ga(7) in Fig. 3) was removed as Ga⁺. Optimization of the

Table 2 Selected distances [pm] for **10a**

Ga(3)–Ga(4)	255.6	Ga(2)–Ga(6)	278.0
Ga(2)–Ga(3)	259.8	Ga(1)–Ga(6)	264.7
Ga(1)–Ga(2)	267.9	Ga(7)–Ga(6)	266.1
Ga(1)–Ga(7)	259.7	Ga(8)–Ga(9)	277.9
Ga(7)–Ga(8)	268.2	Ga(2)–Ga(9)	279.4
Ga(4)–Ga(8)	259.9	Ga(1)–Ga(9)	266.0
Ga(2)–Ga(8)	310.8	Ga(7)–Ga(9)	264.7
Ga(4)–Ga(5)	270.3	Ga(5)–Ga(6)	254.5
Ga(3)–Ga(5)	270.1	Ga(9)–Ga(10)	254.4
Ga(2)–Ga(5)	277.0		
Ga(5)–Ga(8)	276.3	Ga(4)–Si(3)	244.2
Ga(4)–Ga(10)	270.3	Ga(3)–Si(2)	244.1
Ga(3)–Ga(10)	269.9	Ga(5)–Si(4)	244.7
Ga(2)–Ga(10)	276.0	Ga(1)–Si(1)	243.8
Ga(8)–Ga(10)	277.5	Ga(7)–Si(5)	243.9
Ga(6)–Ga(8)	279.4	Ga(10)–Si(6)	244.8

Table 3 Selected distances [pm] for **12a**

Ga(3)–Ga(4)	261.6	Ga(1)–Ga(9)	256.6
Ga(2)–Ga(3)	254.7	Ga(1)–Ga(8)	249.2
Ga(1)–Ga(2)	295.7	Ga(5)–Ga(8)	247.7
Ga(1)–Ga(5)	318.6	Ga(7)–Ga(10)	248.5
Ga(4)–Ga(5)	254.7	Ga(7)–Ga(8)	297.9
Ga(4)–Ga(6)	261.7	Ga(1)–Ga(10)	292.0
Ga(3)–Ga(6)	269.0	Ga(9)–Ga(10)	251.8
Ga(1)–Ga(6)	290.1	Ga(6)–Ga(7)	300.9
Ga(5)–Ga(6)	259.7		
Ga(2)–Ga(6)	285.1		
Ga(4)–Ga(7)	265.2	Ga(3)–Si(1)	244.0
Ga(3)–Ga(7)	274.9	Ga(4)–Si(2)	244.8
Ga(2)–Ga(7)	310.8	Ga(6)–Si(3)	244.7
Ga(1)–Ga(7)	296.7	Ga(8)–Si(4)	245.0
Ga(5)–Ga(7)	283.4	Ga(9)–Si(5)	242.7
Ga(2)–Ga(9)	250.0	Ga(10)–Si(6)	244.4

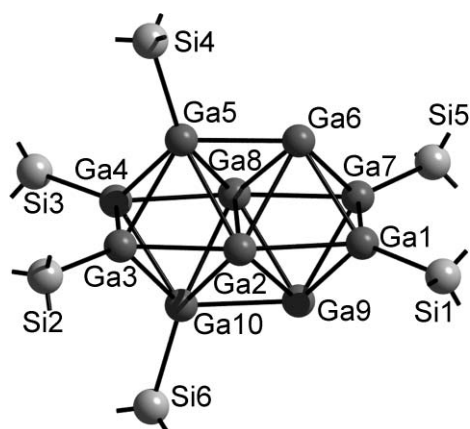


Fig. 2 RI-DFT calculated structure for **10a**. For selected distances see Table 2.

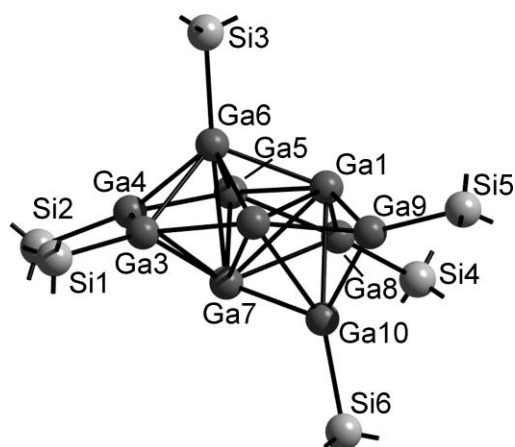


Fig. 3 RI-DFT calculated structure for **12a**. For selected distances see Table 3.

structure of this open $[\text{Ga}_6(\text{SiMe}_3)_6]^-$ cage resulted in **7a** (Fig. 4, Table 4). This represents a structure found for **7**. An assumed formation of **12a** from **7a** (eqn (2))



is exothermic.

Thus, the postulated formation pathways of Ga_{10} clusters (Scheme 2) seem possible. The calculated distances in **10a**, **12a** and **7a** resemble those observed for **10**, **12** and **7** very well. Slight differences are due to the more bulky substituents in **7** and **10**–

Table 4 Selected distances [pm] for **7a**

Ga(3)–Ga(4)	250.0	Ga(1)–Ga(7)	274.7
Ga(2)–Ga(3)	245.4	Ga(5)–Ga(7)	291.2
Ga(1)–Ga(2)	287.4	Ga(2)–Ga(8)	240.5
Ga(1)–Ga(5)	287.7	Ga(1)–Ga(8)	244.0
Ga(4)–Ga(5)	245.5	Ga(1)–Ga(9)	243.9
Ga(4)–Ga(6)	277.1	Ga(5)–Ga(9)	240.7
Ga(3)–Ga(6)	269.8		
Ga(2)–Ga(6)	289.7	Ga(4)–Si(2)	243.6
Ga(1)–Ga(6)	270.5	Ga(3)–Si(1)	243.7
Ga(5)–Ga(6)	282.5	Ga(6)–Si(3)	244.6
Ga(4)–Ga(7)	268.7	Ga(7)–Si(4)	243.8
Ga(3)–Ga(7)	276.5	Ga(8)–Si(5)	243.9
Ga(2)–Ga(7)	283.8	Ga(9)–Si(6)	244.4

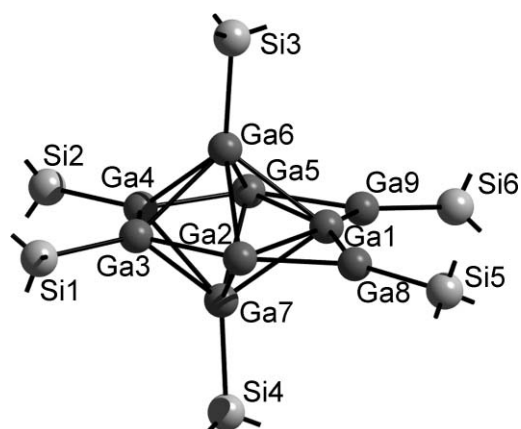


Fig. 4 RI-DFT calculated structure for **7a**. For selected distances see Table 4.

12. If the calculations are done with smaller substituents like SiH_3 , the deviations are much larger and interactions of Si–H bonds with the cluster core occur. A population analysis using the Ahlrichs–Heinzmann method^{35,36} for **12a** reveals intensive multi center bonding based on shared electron numbers (SEN) (see ESI†). An electron–orbital balance makes a description of the bonding in the cluster core of two Ga–Ga 2c2e bonds and ten 3c2e GaGaGa bonds plausible. Three of them are on the faces of the tetrahedral part of the cluster. High two-centre $[\text{Ga}(6)\text{–}\text{Ga}(7)]$ 0.91] and three-centre SENs $[\text{Ga}(1)\text{–}\text{Ga}(6)\text{–}\text{Ga}(7)]$ 0.43] indicate interaction between the apical atoms of the core. The small SEN for the Ga(6)–Si bond (1.0 compared to 1.2 for the others) is due to the high coordination number of seven for the apical gallium atom. Inspecting the HOMO for **12a** (Fig. 5), the different contribution of the bare gallium atoms becomes apparent. Whilst Ga(1), Ga(2) and Ga(7) are engaged in cluster bonding, at Ga(5) the MO has lone pair character. This justifies the electron count applied above. The variation in the bond lengths of the Ga–Si bonds is smaller than in the experimental structure. This is explained by the more bulky substituents and the disorder in the cluster (Experimental section).

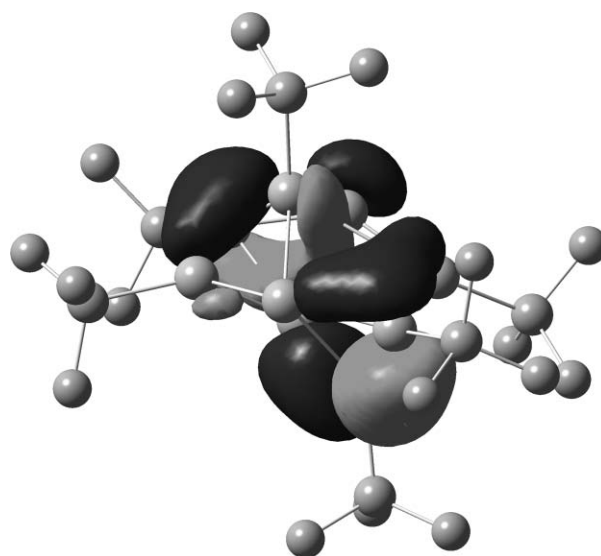


Fig. 5 HOMO for **12a**.

A formally one electron reduction of **12a** gives anionic **13⁻** (eqn (3)).



This is accompanied by a drastic structural change (Fig. 6, Table 5). Further reduction (eqn (4))



is accompanied by minor structural changes, only.

13⁻ and **13²⁻** have core structures that differ only in detail and are very similar to **11**. This means six GaR units form an elongated trigonal antiprism with an intercalated four-membered

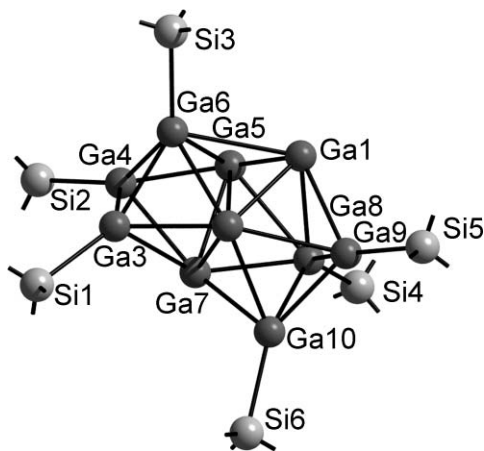


Fig. 6 RI-DFT calculated structure for **13⁻** [**13²⁻**]. For distances see Table 5.

Table 5 Selected distances [pm] for **13⁻**, **13²⁻** (experimental values for **11**)

	13⁻	13²⁻	11
Ga(3)–Ga(4)	254.4	276.4	(269.7)
Ga(2)–Ga(3)	267.3	264.3	(250.2)
Ga(1)–Ga(2)	270.7	310.8	(253.8)
Ga(1)–Ga(5)	249.6	299.2	(245.3)
Ga(4)–Ga(5)	264.5	266.2	(253.7)
Ga(4)–Ga(6)	257.5	250.6	(271.1)
Ga(3)–Ga(6)	274.5	261.7	(269.7)
Ga(2)–Ga(6)	265.2	357.5	(312.2)
Ga(1)–Ga(6)	280.1	252.2	(287.5)
Ga(5)–Ga(6)	277.7	301.6	(321.0)
Ga(4)–Ga(7)	280.7	259.7	(260.6)
Ga(3)–Ga(7)	272.9	260.1	(262.9)
Ga(2)–Ga(7)	268.7	310.7	(245.3)
Ga(2)–Ga(5)	350.2	298.6	(407.7)
Ga(5)–Ga(7)	266.5	299.2	(253.8)
Ga(2)–Ga(8)	270.9	265.5	(253.7)
Ga(1)–Ga(9)	254.5	251.0	(260.6)
Ga(1)–Ga(8)	276.9	261.8	(262.9)
Ga(5)–Ga(8)	299.6	289.9	(250.2)
Ga(7)–Ga(10)	262.3	253.9	(287.5)
Ga(2)–Ga(10)	284.0	312.9	(321.0)
Ga(9)–Ga(10)	263.8	253.7	(271.1)
Ga(8)–Ga(10)	255.7	259.0	(269.7)
Ga(7)–Ga(8)	266.6	268.0	(269.7)
Ga(8)–Ga(9)	263.7	280.6	(269.7)
Ga(4)–Si(2)	243.3	243.5	(247.5)
Ga(3)–Si(1)	245.0	246.0	(249.2)
Ga(6)–Si(3)	243.6	243.7	(247.5)
Ga(10)–Si(6)	244.7	244.5	(247.5)
Ga(9)–Si(5)	243.2	243.1	(247.5)
Ga(8)–Si(4)	243.4	245.6	(249.2)

ring of gallium atoms. A comparison with the experimental values for **11** is difficult, because in **11** the cluster core is severely disordered. Bearing in mind the difference in the steric demand of the substituents, **13⁻** and **11** are in good agreement (atom numbering according to Fig. 1). The transition from **12a** to **13⁻** may be described as moving atom Ga1 out of the equatorial plane of the pentagonal bipyramid, which results in a elongation of the Ga(1)–Ga(6) bond and shortening of the Ga–Ga bonds between the GaR units.

Experimental

All experiments were performed under purified nitrogen or in vacuum with Schlenk techniques. NMR: Bruker AXS 200. Mass spectra: Finnegan MAT 8400. X-Ray crystallography: a suitable crystal was mounted with a perfluorinated polyether oil on the tip of a glass fibre and cooled immediately on the goniometer head. Data collection was performed on a STOE IPDS diffractometer with MoK α radiation ($\lambda = 0.71073 \text{ \AA}$). The structure was solved and refined with the Bruker AXS SHELXTL 5.1 program package. Refinement was full matrix against F^2 . All hydrogen atoms were included as riding models with fixed isotropic U values in the final refinement. For further data see Table 1. The relatively high residual electron density (2.29/–0.81) may be explained by a disorder in the cluster core. Refinement in a split model gave 10 occupation factors of 0.86/0.14 for the gallium positions, but did not result in a significant change in R values. The crystals of **12** were weakly diffracting and no intensity was observed at angles higher than $2\theta = 45^\circ$. Quantum chemical calculations: All DFT calculations have been performed with the TURBOMOLE package³⁶ using RI approximation with BP86 functional and a def-SV(P) basis, as well as Gaussian 03.³⁷

C₇₂H₁₆₂Ga₁₀Si₆ · C₄₈H₁₀₈Ga₄Si₄ (12·1c)

A solution of Na(thf)₂Si(CMe₃)₃ (3.0 g, 8.0 mmol) in 40 ml of toluene was added dropwise to a suspension of “GaI” (1.47 g, 7.5 mmol) in 30 ml of toluene at -78°C . The mixture was warmed to ambient temperature and stirred for further 12 h. All volatiles were removed *in vacuo* and the residue was extracted with 50 ml of pentane. The remaining solid was treated with 40 ml of toluene. From the pentane solution violet crystals of **1c** (NMR, mass spectra are in agreement with those reported in the literature⁴) could be obtained at -30°C . From the toluene solution, after reduction of the volume to 10 ml, black prisms of **12·1c** crystallized at -30°C , yield: 0.15 g (together with crystals of **1c**, **9**, **11**), mp: 70–130 $^\circ\text{C}$ (decomp.). NMR (C₆D₆): $\delta^1\text{H} = 1.37$ (s, CMe₃, **1c**); $\delta^{13}\text{C} = 32.7$ (CMe₃), 26.6 (CMe₃); signals for **12** could not be observed. (Crystals of **12·1c** are of low solubility in common solvents, which was observed for many other higher gallium clusters, too. Thus, NMR spectra are dominated by the soluble **1c**.) MS (EI): m/z 1216 ($\{\mathbf{12} - \text{Ga}_4[\text{Si}(\text{CMe}_3)_3]_2\}^+$), 1076/100, $\mathbf{1c}^+$), 1015 (20, $\{\mathbf{12} - \text{Ga}_4[\text{Si}(\text{CMe}_3)_3]_3\}^+$), 877 (50, $\{\mathbf{1c} - \text{Si}(\text{CMe}_3)_3\}^+$).

Conclusions

During the past decade gallium rich cluster compounds, sometimes apostrophied as metalloidal clusters, have been prepared with cluster cores of 7 to 84 gallium atoms. With the structural

characterization of the neutral decagallane(6) **12** the family of $[\text{Ga}_{10}\text{R}_6]^{n-}$ clusters [$n = 0, 1, \text{R} = \text{Si}(\text{SiMe}_3)_3, \text{C}(\text{SiMe}_3)_3$] became unique in showing polymorphism of the cluster core structure keeping the number of substituents constant.

Structural variety has been observed for Ga_{22} clusters, too. Here, this is made possible by a variation in the degree of substitution, which ranges from eight to twenty. In contrast to the accumulated knowledge on structures of these compounds, their formation pathways have not been revealed, yet.

The topological relationship of the Ga_{10}R_6 cluster family to anionic Ga_8 and Ga_9 clusters is hinted at here. Supporting quantum chemical calculations indicate these assumed formation pathways to be realistic. Obviously, this does not mean that cluster synthesis will be straightforward now, but it might be a tiny step directed to an understanding of the formation of these unusual compounds. A practical handicap in these investigations is that the clusters are obtained only in minor yields by the present methods. Therefore effort has to be made to find more effective starting materials for low valent gallium compounds.

Acknowledgements

We are grateful to the Deutsche Forschungsgemeinschaft for financial support. We also thank Mr P. Butzug for assistance in collecting the data sets.

Notes and references

- G. Linti, H. Schnöckel, W. Uhl and N. Wiberg, in *Molecular Clusters of the Main Group Elements*, ed. M. Driess and H. Nöth, Wiley-VCH, Weinheim, Editon edn., 2004, pp. 126–168.
- W. Uhl, W. Hiller, M. Layh and W. Schwarz, *Angew. Chem.*, 1992, **104**, 1378–1380, (*Angew. Chem., Int. Ed. Engl.*, 1992, **31**, 1394–1396).
- G. Linti, *J. Organomet. Chem.*, 1996, **520**, 107–113.
- N. Wiberg, K. Amelunxen, H. W. Lerner, H. Nöth, W. Ponikwar and H. Schwenk, *J. Organomet. Chem.*, 1999, **574**, 246–251.
- G. Linti, S. Çoban and D. Dutta, *Z. Anorg. Allg. Chem.*, 2004, **630**, 319–323.
- A. Schnepf, G. Stöber and H. Schnöckel, *Z. Anorg. Allg. Chem.*, 2000, **626**, 1676–1680.
- W. Uhl, L. Cuyppers, K. Harms, W. Kaim, M. Wanner, R. Winter, R. Koch and W. Saak, *Angew. Chem.*, 2001, **113**, 589–591, (*Angew. Chem., Int. Ed.*, 2001, **40**, 566–569).
- W. Uhl, L. Cuyppers, W. Kaim, B. Schwederski and R. Koch, *Angew. Chem.*, 2003, **115**, 2524–2526, (*Angew. Chem., Int. Ed.*, 2003, **42**, 2422–2424).
- K. Wade, *Adv. Inorg. Chem. Radiochem.*, 1976, **18**, 1–66.
- R. W. Rudolph, *Acc. Chem. Res.*, 1976, **9**, 446–452.
- R. E. Williams, *Adv. Inorg. Chem. Radiochem.*, 1976, **18**, 67–142.
- D. M. P. Mingos, *Nature*, 1972, **236**, 99–102.
- K. Wade, *J. Chem. Soc. D*, 1971, 792–793.
- D. M. P. Mingos, *Acc. Chem. Res.*, 1984, **17**, 311–319.
- N. Wiberg, T. Blank, H. Nöth, M. Suter and M. Warchold, *Eur. J. Inorg. Chem.*, 2002, **4**, 929–934.
- G. Linti and W. Köstler, *Angew. Chem.*, 1997, **109**, 2758–2560, (*Angew. Chem., Int. Ed. Engl.*, 1997, **36**, 2644–2646).
- A. Schnepf, G. Stöber, R. Köppe and H. Schnöckel, *Angew. Chem.*, 2000, **112**, 1709–1711, (*Angew. Chem., Int. Ed.*, 2000, **39**, 1637–1639).
- M. Kehrwald, W. Köstler, G. Linti, A. Rodig, T. Blank and N. Wiberg, *Organometallics*, 2001, **20**, 860–867.
- H. Schnöckel, *Dalton Trans.*, 2005, **19**, 3131–3136.
- A. Schnepf, E. Weckert, G. Linti and H. Schnöckel, *Angew. Chem.*, 1999, **111**, 3578–3581, (*Angew. Chem., Int. Ed.*, 1999, **38**, 3381–3383).
- G. Linti and A. Rodig, *Chem. Commun.*, 2000, 127–128.
- A. Donchev, A. Schnepf, G. Stöber, E. Baum, H. Schnöckel, T. Blank and N. Wiberg, *Chem.–Eur. J.*, 2001, **7**, 3348–3353.
- A. Schnepf, G. Stöber and H. Schnöckel, *Angew. Chem.*, 2002, **114**, 1959–1962, (*Angew. Chem., Int. Ed.*, 2002, **41**, 1882–1884).
- A. Schnepf, R. Köppe, W. Weckert and H. Schnöckel, *Chem.–Eur. J.*, 2004, **10**, 1977–1981.
- J. Steiner, G. Stöber and H. Schnöckel, *Angew. Chem.*, 2004, **116**, 6712–6715, (*Angew. Chem., Int. Ed.*, 2004, **43**, 6549–6552).
- M. L. H. Green, P. Mountford, G. J. Smout and S. R. Speel, *Polyhedron*, 1990, **9**, 2763–2765.
- N. Wiberg, *Coord. Chem. Rev.*, 1997, **163**, 217–252.
- R. B. King, *Inorg. Chim. Acta*, 1996, **252**, 115–121.
- Z. X. Wang and P. v. R. Schleyer, *Angew. Chem.*, 2002, **114**, 4256–4259, (*Angew. Chem., Int. Ed.*, 2002, **41**, 4082–4085).
- S. C. Sevon and J. D. Corbett, *Inorg. Chem.*, 1991, **30**, 4875–4877.
- R. B. King, *J. Organomet. Chem.*, 2002, **646**, 146–152.
- M. M. Baslarkrishnarajan and E. D. Jemmis, *J. Am. Chem. Soc.*, 2000, **122**, 4516–4517.
- E. D. Jemmis, M. M. Baslarkrishnarajan and P. D. Pancharatna, *J. Am. Chem. Soc.*, 2001, **123**, 4313–4323.
- O. Treutler and R. Ahlrichs, *J. Chem. Phys.*, 1995, **102**, 346–354.
- R. Heinzmann and R. Ahlrichs, *Theor. Chim. Acta*, 1976, **42**, 33–45.
- R. Ahlrichs and C. Ehrhardt, *Chem. Unserer Zeit*, 1985, **19**, 120–124.
- M. J. Frisch, G. W. Trucks, H. B. Schlegel, G. E. Scuseria, M. A. Robb, J. R. Cheeseman, J. A. Montgomery, Jr., T. Vreven, K. N. Kudin, J. C. Burant, J. M. Millam, S. S. Iyengar, J. Tomasi, V. Barone, B. Mennucci, M. Cossi, G. Scalmani, N. Rega, G. A. Petersson, H. Nakatsuji, M. Hada, M. Ehara, K. Toyota, R. Fukuda, J. Hasegawa, M. Ishida, T. Nakajima, Y. Honda, O. Kitao, H. Nakai, M. Klene, X. Li, J. E. Knox, H. P. Hratchian, J. B. Cross, C. Adamo, J. Jaramillo, R. Gomperts, R. E. Stratmann, O. Yazyev, A. J. Austin, R. Cammi, C. Pomelli, J. W. Ochterski, P. Y. Ayala, K. Morokuma, G. A. Voth, P. Salvador, J. J. Dannenberg, V. G. Zakrzewski, S. Dapprich, A. D. Daniels, M. C. Strain, O. Farkas, D. K. Malick, A. D. Rabuck, K. Raghavachari, J. B. Foresman, J. V. Ortiz, Q. Cui, A. G. Baboul, S. Clifford, J. Cioslowski, B. B. Stefanov, G. Liu, A. Liashenko, P. Piskorz, I. Komaromi, R. L. Martin, D. J. Fox, T. Keith, M. A. Al-Laham, C. Y. Peng, A. Nanayakkara, M. Challacombe, P. M. W. Gill, B. Johnson, W. Chen, M. W. Wong, C. Gonzalez and J. A. Pople, *GAUSSIAN 03*, Gaussian, Inc., Pittsburgh, PA, Editon edn., 2003.